



Simulation of storm surge inundation under different typhoon intensity scenarios: Case study of Pingyang County, China

5 Xianwu Shi^{1,3}• Pubing Yu²• Zhixing Guo¹• Fuyuan Chen²• Xiuguang Wu²• Zhilin Sun³• Wenlong Cheng²• Jian Zeng²

¹National Marine Hazard Mitigation Service, Beijing, 100194, China

²Zhejiang Institute of Hydraulics and Estuary, Hangzhou, 310020, China

³Zhejiang University, Hangzhou, 310058, China

Correspondence to: Jian Zeng(zengi-1000@163.com)

10 **Abstract:** China is one of the countries that are most seriously affected by storm surges. In recent years, storm surges in coastal areas of China have caused huge economic losses and a large number of human casualties. Knowledge of the inundation range and water depth of storm surges under different typhoon intensities could assist pre-disaster risk assessment and making evacuation plans, as well as provide decision support for responding to storm surges. Based on historical typhoon-induced storm surges in
15 the study area of Pingyang County in Zhejiang Province, China, key parameters including typhoon tracks, radius of maximum wind speed, astronomical tide, and upstream flood runoff were determined for different typhoon intensities. Numerical simulations were conducted using these parameters to investigate the inundation range and water depth distribution of storm surges in Pingyang County under five different intensity scenarios (915, 925, 935, 945, and 965 hPa) with consideration of the impact of
20 seawall collapse. The simulation results show that the range of storm surge inundation expands with increasing typhoon intensity. The scenario with the most intense typhoon (915 hPa) had the most adverse track, with an associated area of inundation of 233 km² that included most areas of the town of Aojiang, eastern areas of Wanquan, northern areas of Songbu, as well as parts of Kunyang and Shuitou.

Keywords: Intensity scenarios; Inundation simulation; Pingyang County; Typhoon-induced storm surge

25 1 Introduction

China is among the few countries affected seriously by storm surges. A storm surge can cause overflow of tide water and seawall destruction that can result in flooding in coastal areas, which can be extremely destructive and can have serious impact on surrounding areas (Sun et al. 2015). Storm surges have occurred along much of China's coast from south to north (Gao et al. 2014). On average, approximately
30 nine typhoons annually make landfall over China (Shi et al. 2015), most of which cause storm surges. In 2018, storm surge disasters caused coastal flooding in China that resulted in 3 deaths and direct economic losses of RMB 4.456 billion (Ministry of Natural Resources 2019). With the recent rapid socioeconomic development in China, industrialization and urbanization processes in coastal areas have accelerated, and both the population density and the social wealth in such areas have increased sharply. Concurrently,
35 owing to global climate change and sea level rise, the occurrence of weather situations that trigger storm surges has become more frequent and the associated risk level of coastal storm surges has increased significantly (Fang et al., 2014; Yasser et al., 2018). Fortunately, the number of fatalities in China due to



40 storm surges has decreased significantly because of improvements in the regional early warning capability (Shi et al. 2015). Thus, the focus on storm surge disasters has changed from reduction of disaster losses to mitigation of disaster risks. Therefore, increasing importance has been attached to studies on storm surge risk (Shi et al., 2019).

45 Storm surge risk assessment estimates the risk level of future storm surges in a certain region based on deterministic numerical simulation in combination with designed probabilistic storm surge scenarios (Shi et al. 2013; Wang et al. 2018). The calculation of storm surge under scenarios with storms of different intensity is an important part of storm surge risk assessment. The calculation results could provide important decision-making support for the planned response to storm surges in coastal areas, and they could assist in both the pre-assessment of storm surge disasters and the preparation of storm surge emergency evacuation plans. Following the earthquake-induced “3.11” tsunami that occurred in Japan in 2011, scientific research on many aspects of marine disaster risk management became of great concern to various governments. With consideration of storm surge disaster as the primary hazard, China commenced a project for marine disaster risk assessment and zoning, and it subsequently released its marine industry standard, *the Technical Guidelines for Risk Assessment and Zoning of Marine Disaster Part 1: Storm Surge* (Liu et al. 2018). Calculation of the inundation range and water depth of storm surges associated with typhoons of different intensity is one of the most important tasks in storm surge risk assessment.

55 The core element of simulation of inundation by storm surge disaster under scenarios of different typhoon intensity is to set key parameters for both the typhoons and the storm tides (e.g., typhoon track, typhoon intensity, radius of maximum wind speed, and astronomical tide) under different conditions. Wang (2002) calculated the maximum possible land inundation range based on the translation speed of various historical typhoons (category: 3–5) in the study area, in combination with the SLOSH numerical model. A universal product for the determination of inundation range and water depth distribution for typhoons of different intensity was developed, and it was concluded that storm surges caused by category 5 typhoons would be the probable maximum storm surge. Tomohiro et al. (2010) set key parameters for the largest possible typhoon-induced storm surge in different regions of Japan by simulating typhoon track translation using indicators of the Ise Bay typhoon (the most serious typhoon event recorded in Japan’s history) as reference typhoon parameters. This method is of wide applicability and it is easy to implement; however, it also has certain limitations attributable to its dependence on the availability of recorded information on historical storm surge events. To overcome this problem, a complete method has gradually been developed for stochastic simulation of typhoon track and intensity. The main idea of such a method is to analyze the statistical probability characteristics of historical typhoons in terms of their annual frequency, seasonal distribution, track distribution, intensity, and range of influence range. Based on these features, the generation, development, and extinction of typhoons can be simulated to generate a large number of complete event samples of typhoon track and intensity (Powell et al., 65 70 75 2005; Lin et al., 2010). By selecting events with different typhoon intensity from the generated



samples, the inundation range and water depth in a study area can be calculated using a numerical model of storm surges (Wood et al. 2006; Wahl et al. 2015). This study considered Pingyang County of Zhejiang Province (China) as the target area. The objective was to propose a technical method on setting key parameters (e.g., typhoon track, maximum wind speed radius, astronomical tide, and upstream flood runoff) of typhoon-induced storm surge, and to calculate the inundation range and water depth distribution caused by different typhoon intensity scenarios.

2 Case study area

Pingyang County is a coastal county belonging to the city of Wenzhou in Zhejiang Province, China (Figure. 1) and is affected most frequently by storm surge in coastal areas. It is located in the tropical storm zone of the western Pacific Ocean and is generally exposed to the risk of storm surges during July–October. Pingyang County lies within the region $27^{\circ}21'–27^{\circ}46'N$, $120^{\circ}24'–121^{\circ}08'E$, and it is bordered by Ruian, Wencheng, Taishun, and Cangnan counties. The county extends roughly 83 km from East–West and roughly 25.4 km from North–South, covering an area of approximately 1051 km². It is a highly developed and densely populated area of China with considerable asset exposure. Pingyang County has a population of approximately 800,000, and it is the first National Coastal Economic Open County with customs, ports, and important industries. The coastal zone of Pingyang County, which extends for 22 km, is surrounded by sea on its eastern, southern, and northern sides. The Aojiang and Feiyun rivers flow across the county and they discharge into the East China Sea. Storm surges frequently hit this county, which is one of the reasons why the China State Oceanic Administration approved Pingyang County as the first National Marine Disaster Mitigation Comprehensive Demonstration Area in China.



Figure. 1 Case study area



3 Establishment of the storm surge numerical model

3.1 Model configuration

100 The storm surge numerical model used in this study, developed by the Zhejiang Institute of Hydraulics
 and Estuary, is based on the unstructured-grid finite volume method, and more detailed model
 information could be found in Chen et al (2019). It has characteristics of high efficiency, accuracy,
 conservation, and automatic capture of intermittent flow. This model could be used to simulate
 conventional river channel flow and offshore water flow including flood evolution, astronomical tides,
 105 storm surges, and flooding. The storm surge simulations were performed in combination with the
 calculation of river runoff and consideration of typhoon wind and air pressure fields. Thus, the model
 was capable of simulating large-scale detailed storm surge flooding. The open-sea boundary of the model
 was set near the first typhoon warning line in China's offshore area. The model contained triangular and
 quadrilateral grids consisting of 258,543 units and 173,910 nodes. The coverage extended to Bohai Bay
 110 and the Sea of Japan in the north, to the south of Taiwan in the south, and to the east of the Ryukyu
 Islands (as shown in Figure. 2a) in the east. The upper boundary of the Aojiang River was set at Daitou,
 the upper boundary of the Feiyun River was at Zhaoshandu, and the upper boundary of the Oujiang River
 was set at Weiren. The grid for the offshore area and land in Pingyang County with elevation of <30 m
 (including Nanji Island) had a side length of 50–200 m, and the minimum side length was 15 m (as shown
 115 in Figure. 2b). The model covered the Bohai Sea, Yellow Sea, East China Sea, Sea of Japan, Korean
 Strait, Taiwan Strait, Yangtze River Estuary, Hangzhou Bay, and Qiantang River. The mesh grid was
 finest in localized areas of the Zhejiang offshore region, Oujiang River Estuary, Feiyun River Estuary,
 and Aojiang River Estuary.

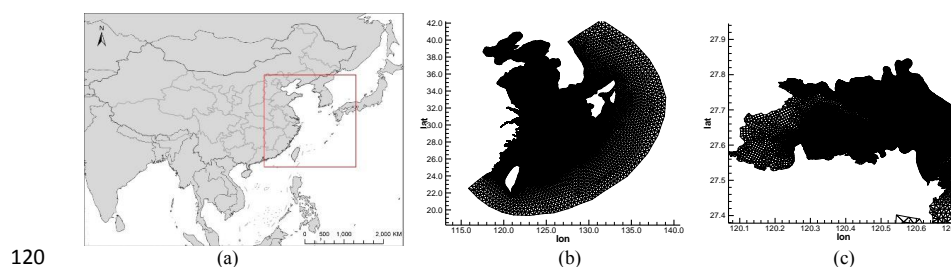


Figure. 2 (a) Model domain with unstructured triangular grids (in red box), (b) mesh of the numerical model in the offshore area, and (c) refined mesh in Pingyang County

3.2 External force

125 The storm surge numerical model was driven by wind stress and the atmospheric pressure gradient acting
 on the surface. The Jelesnianski model was chosen to generate the wind and pressure fields (Jelesnianski,
 1965), for which the calculation formulas are as follows:

$$W = \begin{cases} \frac{r}{r+R} (V_{0x}\vec{i} + V_{0y}\vec{j}) + W_R \left(\frac{r}{R}\right)^{\frac{3}{2}} \frac{(A\vec{i}+B\vec{j})}{r}, & (0 < r \leq R) \\ \frac{R}{r+R} (V_{0x}\vec{i} + V_{0y}\vec{j}) + W_R \left(\frac{R}{r}\right)^{\beta} \frac{(A\vec{i}+B\vec{j})}{r}, & (r > R) \end{cases} \quad (1)$$



$$P_a = \begin{cases} P_0 + \frac{1}{4}(P_\infty - P_0) \left(\frac{r}{R}\right)^3, & (0 < r \leq R) \\ P_\infty - \frac{3}{4}(P_\infty - P_0) \frac{R}{r}, & (r > R) \end{cases} \quad (2)$$

and

$$130 \quad A = -(x - x_c) \sin \theta + (y - y_c) \cos \theta \quad (3)$$

$$B = (x - x_c) \cos \theta + (y - y_c) \sin \theta \quad (4)$$

In the above equations, R is the radius of maximum wind speed, r is the distance from the calculated point to the center of the typhoon, (V_{0x}, V_{0y}) is the translation speed of the typhoon, (x, y) and (x_c, y_c) are the coordinates of the calculated point and the typhoon center, respectively, θ is the inflow angle, P_0 is the central pressure of the typhoon, P_∞ is the atmospheric pressure at infinite distance, and W_R is the maximum wind speed of the typhoon.

135

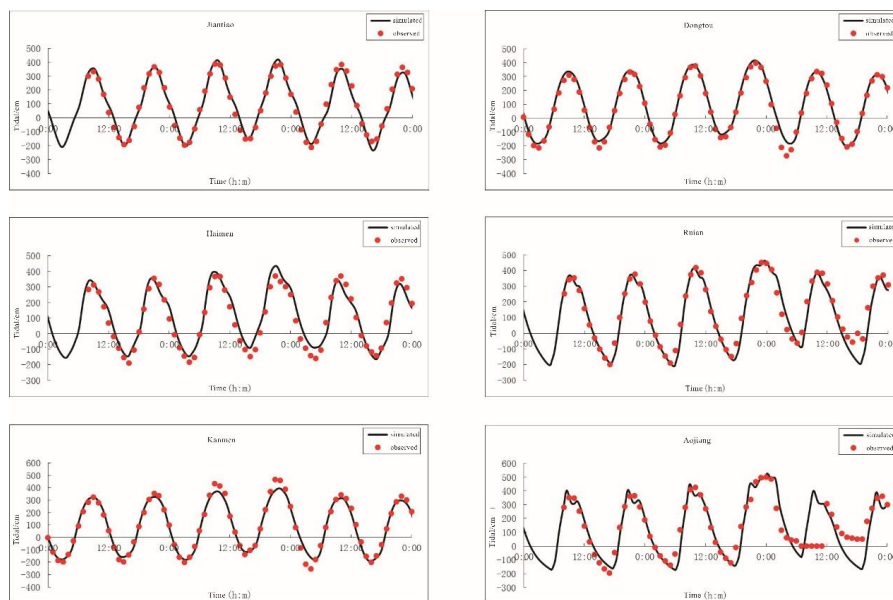
3.3 Model verification

Verification of the storm surge numerical model was performed using 20 typhoon-induced storm surge events that affected Pingyang County during 1990–2015. Error statistics between each of the 20 simulated and observed typhoon processes were compiled in terms of the high tide level (Table 1) and the maximum storm surge (Table 2) at six tidal stations (Jiantiao, Haimen, Kanmen, Dongtou, Ruian, and Minjiang) close to Pingyang County. According to the statistical results, the average error of the high tide level was 14 cm, and 94% of the highest tide level errors were <30 cm. The average error of the high tide level of all involved tidal stations was 12–18 cm, and the average error of the storm surge high tide level of all involved typhoons was 8–25 cm. The average error of the maximum storm surge was 13 cm, and 55% of the maximum storm surge errors were <10 cm or 10% of the maximum storm surge. The average maximum storm surge error of all involved tidal stations was 11–15 cm, and the average error of the maximum storm surge of all involved typhoons was 7–20 cm. Verification of the high tide level and of the storm surge for tidal stations affected by Typhoon Fitow (No. 1323) is presented in Figure. 3 and 4, respectively. It can be seen that both the phase and the high tide level obtained from the storm surge simulation are highly consistent with the actual measurements, proving that the storm surge numerical model developed in this study was reliable.

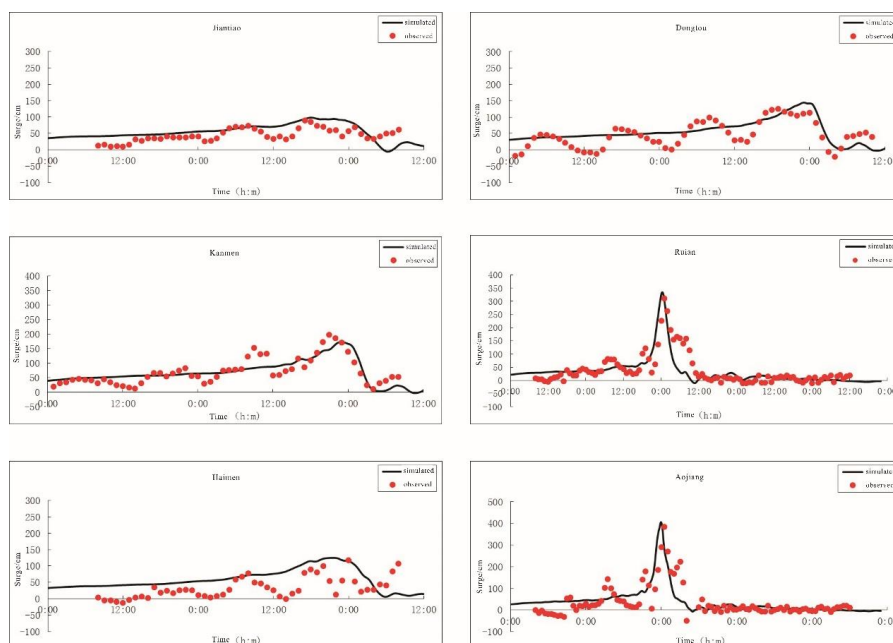
140

145

150



155 **Figure 3** Verification of the high tide level for tidal stations affected by the storm surge caused by Typhoon Fitow (No. 1323)



160 **Figure 4** Verification of the storm surge for tidal stations affected by the storm surge caused by Typhoon Fitow (No. 1323)

165



Table 1 Error statistics in terms of the high tide level during landfall of 20 typical typhoons (unit: cm)

	Jiantiao	Haimen	Kanmen	Dongtou	Ruian	Aojiang	Average
9015	—	—	3	2	-23	—	8
9216	-6	-24	—	-15	-1	4	12
9219	20	23	-1	18	-7	-3	11
9417	14	4	—	31	11	-3	11
9608	-19	-20	—	-30	-25	2	18
9711	-17	11	-24	—	-24	-31	20
0004	16	25	-20	1	14	15	13
0008	12	-1	-26	12	7	13	11
0108	18	14	16	17	24	22	18
0216	5	-16	-11	17	21	17	15
0505	31	-5	-31	-33	-15	31	21
0509	-17	-17	-14	-14	2	7	13
0515	0	28	-17	-4	1	6	11
0604	-2	-14	-24	-9	-17	-1	14
0608	1	-13	-2	3	15	23	9
0713	16	4	10	-1	25	26	15
0716	19	8	14	13	21	15	15
0908	20	22	—	—	10	2	12
1209	6	-10	-21	-10	16	15	13
1323	26	31	-55	19	-8	-17	25
Average	14	15	18	14	14	14	14.8

Note: “—” means no observational value.

170

Table 2 Error statistics in terms of the maximum storm surge during landfall of 20 typical typhoons (unit: cm)

	Jiantiao	Haimen	Kanmen	Dongtou	Ruian	Aojiang	Average
9015	—	—	-11	-17	-9	—	11
9216	-8	-6	-34	-6	-2	-12	11
9219	6	15	-11	14	13	20	13
9417	-21	-17	-2	—	-20	-8	12
9608	-10	-21	-35	-10	-16	-10	15
9711	23	21	-15	-20	-1	-7	17
0004	10	12	-14	7	10	-4	8
0008	3	-2	-2	16	-2	10	7
0108	10	10	1	27	5	3	9
0216	11	2	2	2	26	19	11
0505	-15	-5	-26	-10	-26	-38	20
0509	-8	17	-14	8	-15	-10	11
0515	9	12	-20	-12	-23	-10	12
0604	-10	-21	-35	10	15	9	16
0608	-1	5	10	-13	13	-3	8
0713	21	-2	-8	28	17	18	16
0716	9	15	20	2	17	21	15
0908	-42	-3	—	—	-6	-5	11



1209	—	—	-6	—	10	13	10
1323	5	7	-27	12	21	19	17
Average	12	11	15	13	13	13	13

Note: “—” means no observational value.

4 Parameter setting

4.1 Typhoon intensity

Pingyang County is frequently affected by typhoons. During 1951–2013, the county experienced 132 hazardous typhoons with an average occurrence frequency of 2.13 times per year. Since 1990, the county has been affected by 20 typhoons with central air pressure in the range of 920–985 hPa (average: 965 hPa). Based on the actual needs for response to coastal storm surges, this study considered typhoons with five different levels of intensity (Table 3), which were based on the central air pressure during landfall with reference to the *Technical Guidelines for Risk Assessment and Zoning of Marine Disaster Part 1: Storm Surge* (Liu et al. 2018).

Table 3 Typhoon intensity scenarios

Typhoon Intensity	I	II	III	IV	V
Maximum wind force	Level 12-13	Level 14-15	Level 16	Level 17	Above 17
Minimum air central pressure (hPa)	965	945	935	925	915

4.2 Typhoon track

This study selected the two typhoons that had the most severe impact on Pingyang County and that generated the most significant storm surge in history, i.e., Typhoon Fred (No. 9417) and Typhoon Saomai (No. 0608). Typhoon Fred caused the most severe storm surge in central and southern parts of Zhejiang Province (including Pingyang County) since 1949. The minimum central air pressure of this typhoon was 935 hPa; however, when making landfall near Ruian, the central air pressure was 960 hPa and the radius of maximum wind speed was approximately 50 km. This typhoon landed at the time of the highest astronomical tide and it generated the highest tide level ever recorded in the coastal area. Typhoon Saomai had the lowest central air pressure and the fastest wind speed of any typhoon since 1949. The minimum central air pressure reached 915 hPa; however, when making landfall near the Cangan tidal station, the central air pressure was 920 hPa and the radius of maximum wind speed was approximately 15 km. Before making landfall, both typhoons traveled in a direction perpendicular to the shoreline, conducive to generating the greatest storm surge.

To determine which of these two typhoons had the track that caused the larger storm surge in Pingyang County under the same conditions, both were assumed to have central air pressure of 915 hPa, radius of maximum wind speed of 36 km, and constant direction of movement. The track of Typhoon Fred was translated to the landing site of Typhoon Saomai. The results showed that the maximum storm surge of Typhoon Fred and Typhoon Saomai was 7.22 and 7.47 m, respectively, at Aojiang and 7.00 and 7.03 m, respectively, at Ruian. As the storm surge associated with Typhoon Saomai was slightly larger, the track



of this typhoon was selected as the designed typhoon track. The designed typhoon track was translated to a position in the middle of Pingyang County and then translated to the sides by a distance of 0.25 times the radius of maximum wind speed, until the track combination that maximized the storm surge in each coastal area of Pingyang County was determined. This track was then used for the inundation superposition calculation.

205

4.3 Radius of maximum wind speed

The radius of maximum wind speed of a typhoon is an important factor affecting the magnitude of storm surge. The radius of maximum wind speed of the typhoons selected in this study was calculated using the following empirical relationship:

$$R = R_0 - 0.4(P_0 - 900) + 0.01(P_0 - 900)^2 \quad (5)$$

where P_0 is the central air pressure (hPa), R is the radius of maximum wind speed, and R_0 is an empirical constant. The recommended value is 40, although this can also be adjusted by the fitting accuracy of the air pressure or the wind speed. Thus, the radius of maximum wind speed can be calculated from the central air pressure of the typhoons with five different intensities at the time of landfall, i.e., 56, 42, 38, 36, and 36 km.

215

4.4 Astronomical tide

The coupling of the astronomical tide and the storm surge was performed for simulation of the total elevation and range of inundation. The monthly averaged high tide levels of the previous 19 years during June–October at the representative tidal stations in the study area were selected as the astronomical tide levels that were coupled with the storm surge at peak surge times in the local coastal area. The astronomical tide levels at Dongtou Station on the northern side of Pingyang County and at Pipamen Station on the southern side were 2.46 and 2.33 m, respectively. The larger value of 2.46 m was taken as the astronomical tidal level of the storm surge in the storm surge numerical model for the inundation simulation.

220

4.5 Upstream flood runoff

The upstream flood is a factor required for numerical simulation of storm surges in estuary areas. Analysis of measured data and model studies indicate that the high-water level in an estuary area is controlled mainly by the astronomical tide and the typhoon-induced storm surge. The peak flow in an estuary has no obvious influence on the high-water level during the passage of a typhoon (Sun et al., 2017). The storm surge–runoff interaction in an estuary area increases the tidal level of a typhoon-induced storm surge, resulting in a larger hazard (Zheng et al., 2013). The larger the volume of runoff is, the greater the tidal level in the estuary area will be (Hao et al. 2018). The Feiyun and Aojiang rivers, located on the northern and southern sides of Pingyang County, respectively, are the main rivers that affect the level of flooding in Pingyang County. In this study, the superimposed upstream flood in the numerical simulation of storm surge was the average peak flows in the estuary areas of these rivers in

225

230

235



the period of the selected historical typhoons during April-October, i.e., 1717 and 2348 m³/s for the Aojiang River and Feiyun River, respectively.

4.6 Setting of seawall collapse scenario

240 The seawall is an important barrier against storm surges and excessive overtopping of waves is the main
cause of seawall collapse. Overtopping waves flush the seawall or the landward slope, forming a scour
pit. As the scour pit grows, the upper structure of the seawall loses support and becomes unstable (Sun
et al. 2015; Zhang et al. 2017). In the design of the majority of seawalls in China's coastal areas, the
wave overtopping rate, which is determined based on tide level, wave height, and seawall structure, is
used as a controlling indicator and as a parameter to judge whether a seawall will collapse. According to
245 the results of physical model tests, seawall collapse will occur when the wave overtopping rate of the
coastal seawall in Pingyang County exceeds 0.05 m³/s (Zhejiang Institute of Hydraulics and Estuary
2018). Once seawall collapse is determined in the numerical simulation, it will occur instantaneously
without consideration of its process. After seawall collapse occurs in the numerical simulation, the
ground elevation within the seawall is taken as the shoreline elevation, and the width of seawall collapse
250 is determined by the wave overtopping rate at the representative point on the seawall. Each representative
point represents a section of seawall.

5 Calculation results

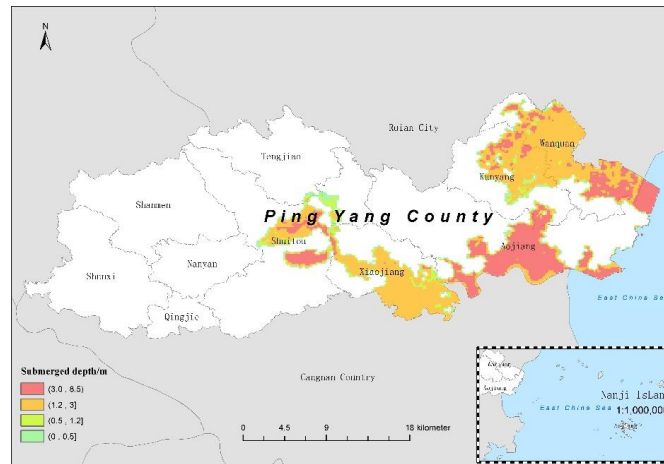
To further analyze the accuracy of the calculation results derived from the simulations, 22 representative
reference points were set along the Pingyang County coast to obtain the desired data (see Fig. 1). The
255 calculated maximum storm surge at each reference point for typhoons of different intensity is shown in
Table 4. It can be seen that for the eastern coastal area of Pingyang County, the maximum storm surge
of the representative points appeared near the radius of maximum wind speed on the southern side of the
point of landfall of the typhoon. For the 915 and 925 hPa super typhoons, the typhoon track was moved
from the reference position of Pingyang (the center of Pingyang County) southward by 25 km, reaching
260 the Feiyun River estuary where the maximum tidal level of 7.78 m appeared; by 30 km, reaching the
Feiyun River estuary and the eastern coast of Pingyang, where the maximum storm tide level of 7.88 m
appeared; and by 40 km, reaching the Aojiang River Estuary, where the maximum storm surge tidal level
of 7.90 m appeared. For the 935, 945, and 965 hPa typhoons, the corresponding maximum storm surge
track moved further southward as the radius of maximum wind speed increased. For example, the 965
265 hPa typhoon should move southward by 89 km from the reference position to reach the eastern coast of
Pingyang, where the maximum tidal level would appear. Overall, the calculated maximum tidal level for
the 925 hPa typhoon was approximately 0.17–0.53 m lower than that of the 915 hPa typhoon, but
approximately 0.29–0.51 m higher than that of the 935 hPa typhoon. The calculated maximum storm
surge tidal level for the 945 hPa typhoon was approximately 0.28–0.5 m lower than that of the 935 hPa
270 typhoon, but approximately 0.71–1.09 m higher than that of the 965 hPa typhoon.

Table 4 Statistical results of maximum tide levels associated with unfavorable tracks of typhoons under different intensity scenarios

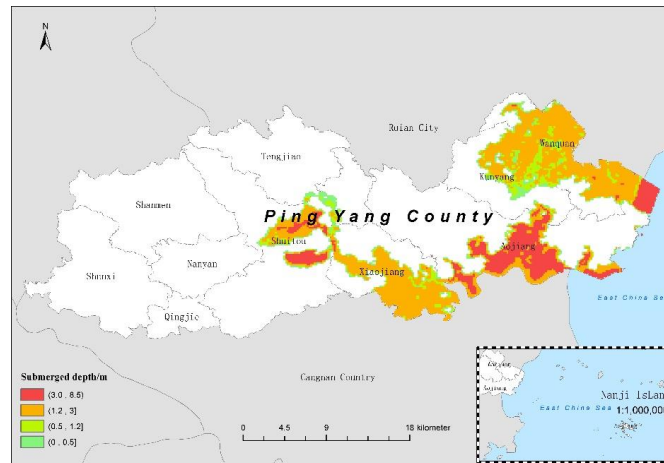


Reference points NO.	915hpa	925hpa	935hpa	945hpa	965hpa
1	7.61	7.28	6.90	6.48	5.53
2	7.59	7.26	6.87	6.46	5.51
3	7.60	7.24	6.85	6.43	5.48
4	7.62	7.24	6.83	6.42	5.46
5	7.65	7.25	6.82	6.40	5.44
6	7.70	7.27	6.82	6.39	5.42
7	7.79	7.32	6.86	6.41	5.42
8	7.85	7.37	6.89	6.44	5.44
9	7.87	7.38	6.90	6.45	5.44
10	7.88	7.38	6.90	6.45	5.44
11	7.88	7.38	6.91	6.45	5.45
12	7.87	7.36	6.90	6.44	5.44
13	7.91	7.39	6.94	6.47	5.46
14	7.58	7.17	6.72	6.27	5.37
15	7.66	7.30	6.84	6.38	5.40
16	7.66	7.43	6.95	6.48	5.45
17	7.79	7.56	7.06	6.58	5.52
18	7.90	7.69	7.18	6.69	5.60
19	7.81	7.62	7.15	6.68	5.68
20	7.64	7.47	7.05	6.64	5.72
21	7.44	7.27	6.91	6.57	5.75
22	7.36	7.05	6.76	6.49	5.77

Storm surge inundation was calculated for the unfavorable tracks corresponding to the five typhoon intensity scenarios. The storm tide levels caused by each unfavorable track were all the maximum storm surges of the 22 representative points around Pingyang. Therefore, it can be considered that the inundation superposition of these unfavorable tracks represented the maximum storm surge inundation range and the water depth distribution in Pingyang County associated with the typhoons of different intensity. The range of inundation in Pingyang County by the storm surges associated with the five typhoons of different intensity is shown in Figure. 6. It can be seen that the inundation range increased with the increase of typhoon intensity. Based on Figure. 6, Table 5 shows the statistical results of the maximum inundated area corresponding to the five typhoon scenarios. It can be seen that the area of Pingyang County inundated by the storm surge associated with the 915 hPa typhoon and the most unfavorable track reached 233 km². The inundated areas included most parts of the town of Aojiang Town, eastern areas of Wanquan, north areas of Songbu, as well as parts of Kunyang and Shitou, including administrative villages such as Qianjie and Jinmei.

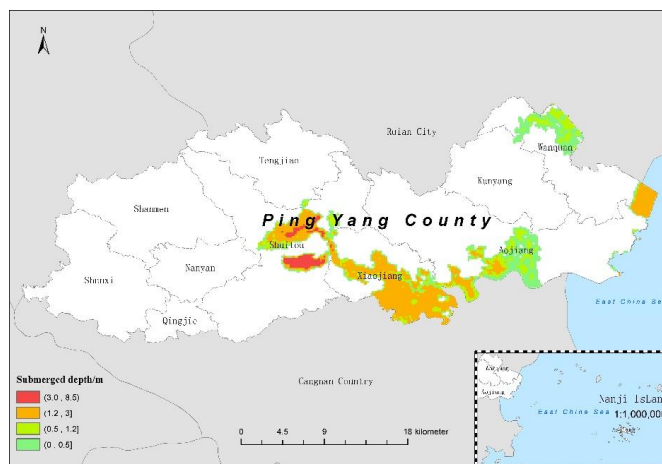


(a)



(b)

290



(e)

Figure 5 Inundation range and water depth distribution of storm surges associated with typhoons of different intensity: (a) 915 hPa, (b) 925 hPa, (c) 935 hPa, (d) 945 hPa, and (e) 965 hPa

300

Table 5 Statistical results of maximum inundated area associated with different typhoon intensity scenarios (unit: km²)

Typhoon Force	>3.0m Class I	1.2–3.0m Class II	0.5–1.2m Class III	Below 0.5m Class IV
915hpa	69.28	144.27	11.75	7.86
925 hpa	44.93	121.10	22.74	10.97
935 hpa	31.68	104.63	40.24	17.03
945 hpa	19.68	97.55	48.33	22.98
965 hpa	5.25	52.54	22.58	23.14

6 Conclusion and discussion

A deterministic method for setting key parameters (e.g., typhoon track, radius of maximum wind speed, astronomical tide, and upstream flood runoff) under different typhoon intensity scenarios for calculation of inundated areas was proposed in this study. It considered Pingyang County as an example, but the developed method could be adopted in all coastal regions. A high-precision numerical model was established and validated for simulating storm surges within the study area. Using these key parameters as driving factors, the inundation range and water depth distribution in Pingyang County corresponding to the storm surges under different typhoon intensity scenarios were simulated in combination with the storm surge numerical model. The simulation results properly reflected the risk distribution attributable to storm surges in Pingyang County. The proposed method could provide reference for the establishment of a technical system for the assessment and zonation of storm surge risk in the coastal counties of China. The inundation range of a storm surge is related to many factors (Petroligkis, 2018). The high-water level in the towns of Shuitou and Xiaojiang in Pingyang County is mainly caused by the upstream flood of the Aojiang River. Consequently, the inundation situation in these two areas is directly related to upstream flood runoff. In this study, the impact of the upstream flood was only considered as the average of the flood peak flow during the storm surge. The water level and inundation range caused by the large

305

310

315



astronomical tide due to the superposition of the extreme flood scenarios might be more unfavorable than
320 the simulated storm surge with the superimposed average of the flood peak runoff, which might result in
uncertainty in the calculation results. In our next study, we will further analyze the quantitative response
relationship between typhoon intensity at landfall and upstream flood runoff, and propose a method for
setting flood runoff upstream of the estuary area.

This paper presents a deterministic method for setting key parameters under typhoon intensity scenarios
325 assuming that these factors (e.g., typhoon track, radius of maximum wind speed, astronomical tide, and
upstream flood runoff) are independent; however, any correlation between these parameters is ignored.
The occurrence probability of parameter combinations is difficult to evaluate. The joint probability
method is an efficient way to determine the base flood elevation due to storm surge (Yang et al. 2019),
and the joint probability among these factors could be established (e.g., using the Copula method) to
330 calculate the occurrence of extreme storm surge events.

This study contributed to the methodology of quantitative assessment of storm surge hazards for coastal
counties. If combined with a vulnerability curve between the loss ratio of typical exposure influenced by
storm surges and the water depth induced by flooding in coastal areas, a quantitative storm surge risk
could be evaluated in future research. The results of a quantitative assessment of storm surge risk could
335 provide a theoretical basis for urban planning, development of emergency evacuation procedures, and
disaster insurance.

Data availability: All data used during the study are available from the corresponding author by request.

Author contribution: Shi prepared the manuscript with contributions from all co-authors and set the
key parameters; Yu, Chen, Wu and Cheng performed the numerical simulation; Guo analyzed the
340 inundated results; Sun provided the tidal observational data; Zeng conducted this research and designed
the experiments.

Competing interests: The authors have declared that no competing interests exist.

Acknowledgments: This work was funded by the National Natural Science Foundation of China
(41701596) and the Open-end Funds of the Key Laboratory of Coastal Disaster and Defense (Hohai
345 University) of the Ministry of Education (201909).

References:

- Chen, F.Y., P.B. Yu, X.G. Wu, and Y.Z. Zhu.: Refined risk assessment of storm surge disaster in coastal
plain: a case study of Pingyang County. *Journal of Tropical Meteorology*, 25(03):304-311,
350 <https://doi.org/10.16555/j.1006-8775.2019.03.002>, 2019.
- Fang, J., Sun, S., Shi, P., and Wang, J.A.: Assessment and Mapping of Potential Storm Surge Impacts on
Global Population and Economy. *International Journal of Disaster Risk Science*, 5(4):323-331,
<https://doi.org/10.1007/s13753-014-0035-0>, 2014
- Gao, Y., Wang, H., Liu, G. M., Sun, X. Y., Fei, X. Y., and Wang, P. T.: Risk assessment of tropical storm
355 surges for coastal regions of China. *Journal of Geophysical Research: Atmospheres*, 119(9):5364-
5374, <https://doi.org/10.1002/2013JD021268>, 2014
- Hao, Z., Hao, F., Singh, V.P., Xia, Y., Shi, C., and Zhang, X.: A multivariate approach for statistical
assessments of compound extremes. *J. Hydrol.* 565, 87–94,
<https://doi.org/10.1016/j.jhydrol.2018.08.025>, 2018.



- 360 Hamdi, Y., Garnier, E., Giloy, N., Duluc, C.M., and Rebour, V.: Analysis of the risk associated with coastal flooding hazards: a new historical extreme storm surges dataset for Dunkirk, France, *Nat. Hazards Earth Syst. Sci.*, 18, 3383–3402, <https://doi.org/10.5194/nhess-18-3383-2018>, 2018.
- Jelesnianski, C.P.: A numerical calculation of storm tides induced by a tropical storm impinging on a continental shelf, *Mon. Weather Rev.* 93(6),343-358, [https://doi.org/10.1175/1520-0493\(1993\)0932.3.CO;2](https://doi.org/10.1175/1520-0493(1993)0932.3.CO;2), 1965.
- 365 Li, Y., Fang, W.H., Lin, W., Ye, Y.T.: Parameterization of synthetic tropical cyclones at various scales for probable maximum storm surge risk modeling. *Marine Sciences*, 38(04):71-80(in Chinese), <https://doi.org/10.11759/hyxx20120829002>, 2014.
- Lin, N., Emanuel, K. A., Smith, J. A., and Vanmarcke, E.: Risk assessment of hurricane storm surge for New York City. *Journal of geophysical research: Atmospheres*, 115(D18). <https://doi.org/10.1029/2009JD013630>. <https://doi.org/10.1029/2009JD013630>, 2010.
- Liu, Q.Z., Shi, X.W., Guo, Z.X.: Technical guidelines for risk assessment and zoning of marine disaster Part 1: Storm surge, Beijing (in Chinese), 2018.
- Ministry of Natural Resources of China.: Chinese marine disaster bulletin of 2018, 2019(in Chinese).
- 375 Petroliaqkis, T. I.: Estimations of statistical dependence as joint return period modulator of compound events – Part 1: Storm surge and wave height, *Nat. Hazards Earth Syst. Sci.*, 18, 1937–1955, <https://doi.org/10.5194/nhess-18-1937-2018>, 2018.
- Powell, M., Soukup, G., Cocke, S., Gulati, S., Morisseau-Leroy, N., and Hamid, S.: State of florida hurricane loss projection model: atmospheric science component. *Journal of Wind Engineering and Industrial Aerodynamics*, 93(8), 651-674. <https://doi.org/10.1016/j.jweia.2005.05.008>, 2005.
- 380 SHI, X.W., FANG, W.H.: Spatiotemporal characteristics of tropical cyclone in NWP basin between 1949 and 2010, *Journal of Beijing Normal University (Natural Science)*, 51(3):287-292(in Chinese). <https://doi.org/10.16360/j.cnki.jbnuns.2015.03.012>, 2015.
- Shi, X.W., Han, Z.Q., Fang, J.Y., Tan, J., Guo, Z.X., and Sun, Z.L.: Assessment and zonation of storm surge hazards in the coastal areas of China. *Natural Hazards*. <https://doi.org/10.1007/s11069-019-03793-z>.
- 385 Shi, X.W., Liu, S., Yang, S.N., Liu, Q.Z., Tan, J., Guo, Z.X.: Spatial-temporal distribution of storm surge damage in the coastal area of China. *Natural Hazards*, 79(1):237-247, <https://doi.org/10.1007/s11069-015-1838-z>, 2015.
- 390 Shi, X.W., Tan, J., Guo, Z.X., and Liu, Q.Z.: A Review of Risk Assessment of Storm Surge Disaster. *Advances in Earth Science*, 28(8):806-874(in Chinese), <https://doi.org/10.11867/j.issn.1001-8166.2013.08.0866>, 2013.
- Sun, Z.L., Huang, S.J., Jiao, J.G., and Nie, H.: Effect of Runoff on Typhoon Storm Surge in Estuaries. *Journal of Tianjin University (Science and Technology)*, 50(5):519-526(in Chinese). <https://doi.org/10.11784/tdxbz201604050>, 2017.
- 395 Sun, Z., Huang, S., Nie, H., Jiao, J., Huang, S., Zhu, L., and Xu, D.: Risk analysis of seawall overflowed by storm surge during super typhoon. *Ocean Engineering*, 107, 178-185. <https://doi.org/10.1016/j.oceaneng.2015.07.041>, 2015.
- Tomohiro, Y., Yuta, T., Nobuhito, M., and Hajime, M.: A Stochastic Typhoon Model Applicable to Storm



- 400 Surge and Wave Simulations for Climate Change Projection. *Journal of Japan Society of Civil Engineers, Ser. B2 (Coastal Engineering)*, 66(1):1241-1245, <https://doi.org/10.2208/kaigan.66.1241>, 2010.
- Wahl, T., Mudersbach, C., and Jensen, J.: Statistical assessment of storm surge scenarios within integrated risk analyses. *Coastal Engineering Journal*, 57(01), 1540003.
- 405 <https://doi.org/10.1142/S0578563415400033>, 2015.
- Wang, X.N.: Risk analysis and simulated of storm surge. *Marine Forecasts*, 19(4):73-76, 2002.
- Wang, Y.X., Duan, Y.H., Guo, Z.X., Chen, W.F., Zhang, X.H., and Han, Z.Y.: Deterministic-probabilistic approach for probable maximum typhoon-induced storm surge evaluation over wenchang in the south china sea. *Estuarine, Coastal and Shelf Science*, 214, 161-172. <https://doi.org/10.1016/j.ecss.2018.09.025>, 2018.
- 410 Wood, R. M., Drayton, M., Berger, A., Burgess, P., and Wright, T.: Catastrophe loss modelling of storm-surge flood risk in eastern england. *Philosophical Transactions of The Royal Society A Mathematical Physical and Engineering Sciences*, 363(1831), 1407-1422. <https://doi.org/10.1098/rsta.2005.1575>, 2005.
- 415 Yang, K., Paramygin, V., Sheng, Y.P.: An objective and efficient method for estimating probabilistic coastal inundation hazards. <https://doi.org/10.1007/s11069-019-03807-w>
- Zhang, Y., Chen, G., Hu, J., Chen, X., Yang, W., Tao, A., and Zheng, J.: Experimental study on mechanism of sea-dike failure due to wave overtopping. *Applied Ocean Research*, 68:171-181. <https://doi.org/10.1016/j.apor.2017.08.009>, 2017.
- 420 Zhejiang Institute of Hydraulics and Estuary. 2018. Research Report on the Influenced Factors of Breakage Volume of Seawall Caused by Storm Surge Disasters (in Chinese).
- Zheng, F. F., Westra, S., Sisson, S.A.: Quantifying the dependence between extreme rainfall and storm surge in the coastal zone. *Journal of Hydrology*, 506(15): 172-187. <https://doi.org/10.1016/j.jhydrol.2013.09.054>, 2013.